Comparison of regional and ecosystem CO_2 fluxes

Sven-Erik Gryning[1], Henrik Soegaard[2] and Ekaterina Batchvarova[3]

[1] Wind Energy Department, Risø National Laboratory for Sustainable Energy, Technical University of Denmark — DTU, DK-4000 Roskilde, Denmark (e-mail: sven-erik.gryning@risoe.dk)
[2] Institute of Geography and Geology, University of Copenhagen, Øster Voldgade 10, DK-1350 København K, Denmark
[3] National Institute of Meteorology and Hydrology, Bulgarian Academy of Sciences, 66 Tzarigradsko Chausse, BG-1784 Sofia, Bulgaria

A budget method to derive the regional surface flux of CO_2 from the evolution of the boundary layer is presented and applied. The necessary input for the method can be deduced from a combination of vertical profile measurements of CO_2 concentrations by i.e. an airplane, successive radio-soundings and standard measurements of the CO_2 concentration near the ground. The method was used to derive the regional flux of CO_2 over an agricultural site at Zealand in Denmark during an experiment on 12–13 June 2006. The regional fluxes of CO_2 represent a combination of agricultural and forest surface conditions. It was found that the regional flux of CO_2 in broad terms follows the behavior of the flux of CO_2 at the agricultural (grassland) and the deciduous forest station. The regional flux is comparable not only in size but also in the diurnal (daytime) cycle of CO_2 fluxes at the two stations.

Introduction

Buffering of fossil CO_2 emissions by the terrestrial and marine ecosystems is essential for the climate. In climate and meteorological models, the individual horizontal grid cells often enclose regions of pronounced inhomogeneities: over land in the vegetation and over the sea in the differential pressure of CO_2 between the air and the sea caused by i.e. biological activity. The estimation of the spatially integrated fluxes is, therefore, a central issue in a large number of scientific, practical and even political assessments of the role of CO_2 emissions for our present and future climate and environment. However, currently it is difficult to measure CO_2 fluxes on the regional scale. As pointed out by e.g. Schlesinger (1983), Cao and Woodward (1998), Huntingford

et al. (2000) and Cramer et al. (2001) this limits our understanding of the interaction between climate change and landuse. This results in a significant uncertainty in the prediction of the future changes in the climate and concentrations of CO_2. Because direct measurements of CO_2 fluxes over inhomogeneous terrain are impractical, indirect approaches are often adapted (Ehleringer and Field 1993, Bouwman 1999).

The mixed layer budget method is an indirect approach that is applicable for the convective boundary layer. It has successfully been applied to estimate surface regional fluxes of sensible and latent heat (e.g. Betts 1973, 1975, 1994, McNaughton and Spriggs 1986, Betts and Ball 1992, Gryning and Batchvarova 1999, Batchvarova et al. 2001). It is rarely used in the context of regional fluxes of CO_2, mainly because pro-

files of CO_2 concentrations in combination with profiles of temperature and wind throughout the convective boundary layer seldom are available. Levy *et al*. (1999) found that the budget method has potential when the CO_2 concentration above the boundary layer can be estimated reliably or measured directly from e.g. airplanes.

The main objective of this study was to explore the feasibility of the version of the budget method, which was developed by Gryning and Batchvarova (1999) for derivation of regional sensible heat fluxes, to estimate the regional fluxes of CO_2. Measurements were drawn from an experimental campaign over Zealand in Denmark carried out in the summer of 2006. We used vertical profiles of CO_2 measured from a research airplane in combination with profiles of wind speed, direction, temperature and water vapor from radiosoundings. The regional fluxes of CO_2 from the budget method were compared with point measurements over grassland and forested areas. Due to technical problems with the airplane only two days of measurements were available for analysis.

Mass balance for CO_2

Here the regional flux of CO_2 is derived from a mass budget for CO_2 extending from the surface to the top of the atmospheric boundary layer, taking into account the entrainment of air above the boundary layer caused by the growth of the boundary layer, as well as the effect of subsidence and the uptake of CO_2 by the vegetation. Following Levy *et al*. (1999) and Denmaed *et al*. (1996) the mass balance is:

$$h\frac{d\chi_{\mathrm{b}}}{dt} = F_{\mathrm{s}} + \left(\chi_{\mathrm{u}} - \chi_{\mathrm{b}}\right)\left(\frac{dh}{dt} - w_{\mathrm{s}}\right) \qquad (1)$$

$$\mathrm{I} \qquad \mathrm{II} \qquad\qquad \mathrm{III} \quad \mathrm{IV}$$

where χ is the scalar concentration, F_{s} is the scalar flux to the surface (positive upward), h is the height of the boundary layer, and w_{s} is the large scale vertical wind velocity at the top of the boundary layer caused by convergence or divergence in the large scale flow field. During synoptic high pressure conditions, w_{s} is negative corresponding to downward motion or subsidence. Subscripts 'b' and 'u' denote quantities within

the boundary layer and in the free air above the boundary layer, respectively. For further analysis it can be broken up into four terms (I–IV). The first term, I, is the change of mass inside the boundary layer, term II is the uptake of CO_2 by the vegetation, term III models the entrainment of CO_2 from air from above the boundary layer caused by the growth of the boundary layer and term IV the effect on the mass budget due to subsidence. The equation can formally be written as:

$$\frac{d\left(h\chi\right)}{dt} = F_{\mathrm{s}} + \chi_{\mathrm{u}}\frac{dh}{dt} - \left(\chi_{\mathrm{u}} - \chi_{\mathrm{b}}\right)w_{\mathrm{s}} \qquad (2)$$

and in discretized form where 1 and 2 is the beginning and end of a time interval

$$\frac{h_2\chi_{\mathrm{b2}} - h_1\chi_{\mathrm{b1}}}{t_2 - t_1} = F_{\mathrm{s}} + \chi_{\mathrm{u}}\frac{h_2 - h_1}{t_2 - t_1} - \left(\chi_{\mathrm{u}} - \chi_{\mathrm{b}}\right)w_{\mathrm{s}} \quad (3)$$

which can be written as

$$\begin{aligned} h_1\chi_{\mathrm{b1}} = h_2\chi_{\mathrm{b2}} - \left(h_2 - h_1\right)\chi_{\mathrm{u}} \\ + \left(\chi_{\mathrm{u}} - \chi_{\mathrm{b}}\right)\left(t_2 - t_1\right)w_{\mathrm{s}} - F_{\mathrm{s}}\left(t_2 - t_1\right) \end{aligned} \qquad (4)$$

Solving for the flux F_{s} at the surface the mass balance can be expressed as

$$\begin{aligned} F_{\mathrm{s}} = \frac{h_1\left(\chi_{\mathrm{u}} - \chi_{\mathrm{b1}}\right) - h_2\left(\chi_{\mathrm{u}} - \chi_{\mathrm{b2}}\right)}{t_2 - t_1} \\ + \left(\chi_{\mathrm{u}} - \chi_{\mathrm{b}}\right)w_{\mathrm{s}} \end{aligned} \qquad (5)$$

The equation, however, does not consider the decrease of air pressure as function of height. The effect can be accounted for by introducing the molar density of air ρ (mol m^{-3}) and the CO_2 mixing ratio C (μmol mol^{-1})

$$\begin{aligned} F_{\mathrm{s}} = \frac{h_1\rho_{\mathrm{b1}}\left(C_{\mathrm{u}} - C_{\mathrm{b1}}\right) - h_2\rho_{\mathrm{b2}}\left(C_{\mathrm{u}} - C_{\mathrm{b2}}\right)}{t_2 - t_1} \\ + \rho_{\mathrm{u}}w_{\mathrm{s}}\left(C_{\mathrm{u}} - C_{\mathrm{b}}\right) \end{aligned} \qquad (6)$$

Ecosystem measurements

Micrometeorological measurements including fluxes and concentration of CO_2 were carried out over an agricultural grassland site near Risø (RIMI) and over a beech forest in the centre of Zealand (Lille Bøgeskov); both monitoring stations are part of the CarboEurope network (Fig.
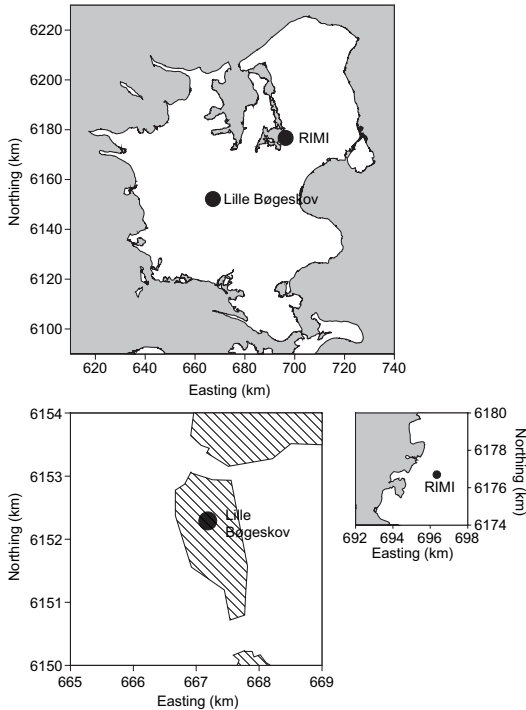
Fig. 1. The position of the two measurement sites on the island of Sealand, Denmark; RIMI (agricultural grassland, white background in the lower right-hand side panel) and Lille Bøgeskov (deciduous forest, slashed-line background in the lower left-hand side panel). The sea is shown in grey.

1). The micrometeorological fluxes were calculated as half-hourly averages by applying the so-called Euroflux methodology, a commonly accepted procedure described in Aubinet *et al.* (2000). The original flow fields were rotated according to the planar fit method (Wilczak *et al.* 2001), and subsequently crosswind- (Liu *et al.* 2001), Moore- (Moore 1986) and Web-corrections (Webb *et al.* 1980) were performed. Dellwik and Jensen (2005) provides details on the treatment of the raw data; corrections (low pass filtering and Webb correction) for closed-path eddy correlation systems measurements of CO_2 are discussed in Ibrom *et al.* (2007a, 2007b). During an intensive measuring campaign on 12–13 June 2006 the measurements of CO_2 profiles were carried out from a research airplane and temperature and wind speed by frequent radio-soundings.

## Lille Bøgeskov

The field station is located at 55°29´13´´N, 11°38´45´´E in a beech forest near Sorø on the island of Zealand. The trees around the station are 82-year old beech (*Fagus sylvatica* L.) with an average tree height of 25 m. The terrain is flat and there is a homogeneous fetch of 0.5 to 1.0 km depending on direction. Flux measurements are performed at 43 meters height. A sonic anemometer SOLENT 1012 R2 measures the 3 components of the wind velocity and temperature. Next to the sonic an inlet to a tube is placed through which air is drawn to an infrared gas analyzes LI-6262 for measurements of fluctuations of concentrations of CO_2 and H_2O.

Pilegaard *et al.* (2003) found that the flux measurements at 43 meters are made in the surface layer of the forest avoiding the roughness sub-layer. Göckede *et al.* (2007) discusses the footprint for the site. By analyzing 2.5 months of data it was found that a high percentage of the measured flux was emitted outside the forest. The effect was most pronounced at westerly and easterly winds (short fetches) and stable conditions. The wind direction and stability dependence of the footprint is illustrated in Göckede *et al.* (2007: fig. 6). It can be seen that during unstable conditions the footprint is covered by the forest with the most favorable conditions at southerly winds — corresponding to a fetch of about 1 km. The experiments discussed here are carried out at southerly winds and the fluxes therefore are considered to be representative for forest conditions.

RIMI

The RIMI field station is situated at 55°41´24´´N, 12°06´36´´E in a rural area 2 km east of Risø National Laboratory. The area is a conventional Danish agricultural area situated in gently rolling terrain with height variations of less than 5 m in a 1-km radius from the site. In 2006 grass was grown on the site. A permanent 10-m mast was instrumented with a sonic anemometer at 2.5-m height (METEK Meteorologische Messtechnik GmbH, Hamburg, Germany) capable of measuring the 3 components of the wind velocity and temperature and an infrared gas analyzer
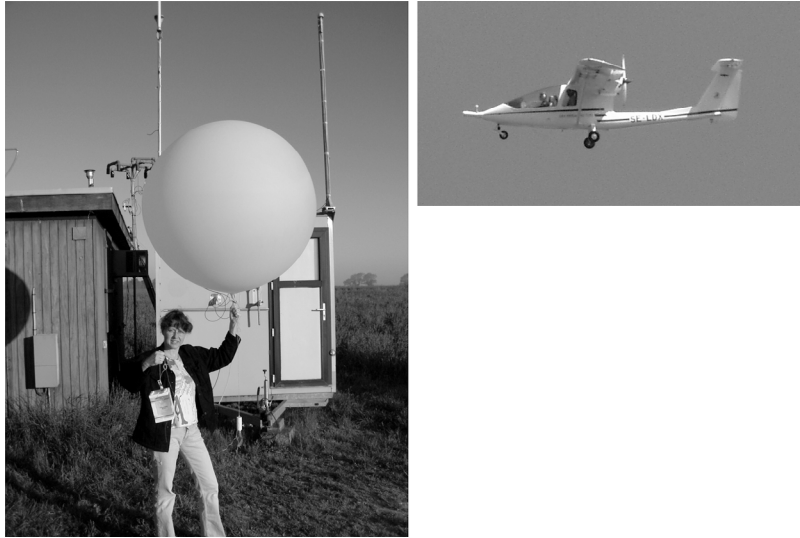
Fig. 2. Pictures from the RIMI site during the experiment. Left-hand picture shows a launch of a radiosonde and the right-hand picture the airplane performing measurements.

LI-6262 for fast measurements of CO_2 and H_2O concentrations. Using the methodology by Soegaard *et al* (2003), it can be seen the footprints for fluxes in unstable atmospheric conditions are well covered by the grassland.

Airplane

A Sky Arrow 650 ERA aircraft (Fig. 2) was used as a platform for measuring vertical profiles over the RIMI site on 12–13 June 2006. The profiles extended from about 100 meters above ground up to 2500 meters. The aircraft carries sensors for measuring a wide variety of atmospheric variables. A platinum resistance device measures air temperature with a frequency of 1 Hz and is used as a low frequency reference. A nose mounted intake connected to a LiCor 7500 open path infrared gas analyzer allowed fast measurements (50 Hz) of CO_2 and H_2O gas concentrations. Unfortunately the GPS (Global Positioning System) on the aircraft was not operating during the flights which made it impossible to determine fluxes. Therefore, only concentrations are used in the present analysis.

Radiosoundings

The height of the boundary layer as function of time was determined experimentally by releas-ing radiosondes (Fig. 2). Sondes were released at 3-h intervals (6:00, 9:00, 12:00, 15:00 and 18:00 local time i.e., GMT + 2). The radiosonde system was made by Modem. The sondes measure temperature with a thermistor, and humidity with a capacitor. A 3D GPS module built into the sonde provides the position, including the height, from which the horizontal wind speed components are derived. Measurements are performed every second.

Results

In order to derive the regional flux of CO_2 to the surface from Eq. 6 the height h of the boundary layer, the vertical velocity w_s of the air in the free atmosphere, the air density ρ_b and CO_2 concentration C_u, above the boundary and near the ground ρ_b and C_b, respectively, should be known as a function of time. Below the derivation of the input parameters is described.

Height of the boundary layer

The height of the boundary layer at the time of each of the radiosounding at the RIMI site was determined (Table 1) subjectively from the measured profiles. Applying objective methods such as the parcel method, based on temperature profiles, recommended by Seibert *et al*. (2000) or

the gradient Richardson number method, based on both temperature and wind speed profiles used by Joffre *et al.* (2001) will inevitably result in different results and furthermore neglect the information on the boundary layer height that can be extracted from other parameters such as the profiles of wind direction as well as humidity. Therefore, in this study the height of the boundary layer was estimated subjectively to the nearest 50 meters by simultaneously considering several parameters in the radiosonde profile such as jumps in the temperature (increase at the top of the boundary layer), shifts in the wind-direction and jumps in the humidity. It is also considered that the turbulence inside the boundary layer is more vigorous as compared with the air above. This effect is seen mainly in the fluctuation of the wind direction but also sometimes in the wind speed.

In order to determine the height of the boundary layer at discrete time intervals for use in Eq. 6, interpolation between the heights of the boundary layer from the radiosoundings was done using the boundary layer expression by Batchvarova and Gryning (1991)

$$\left\{ \frac{h^2}{(1+2A)h-2B\kappa L} + \frac{Cu_*^2}{\gamma \frac{g}{T}\left[(1+A)h-B\kappa L\right]} \right\} \times \left(\frac{dh}{dt} - w_s \right) = \frac{\left(\overline{\theta'w'}\right)_s}{\gamma} \quad (7)$$

Input to the calculation is the surface flux of heat $(\overline{\theta'w'})_s$ and momentum (u_*), which are measured at the RIMI site, as well as the gradient of the potential temperature above the boundary layer (γ) that was determined from the radio-soundings; κ is the von Karman constant, g/T the buoyancy parameter, and A, B and C are parameterization constants (Gryning and Batchvarova 1999). The determination of w_s is discussed in the next chapter.

Large scale vertical motion

The mean large scale vertical motion, w_s, of the air at the top of the boundary layer can be estimated when the horizontal divergence of the large scale flow field

$$\text{div}_{\text{H}} = D^{-1} \int_D \left(\frac{\partial u}{\partial x} + \frac{\partial v}{\partial y} \right) dx\, dy \quad (8)$$

is known as function of height. Here D represents the surface area. For the special case of the horizontal divergence constant with height w_s can be expressed as:

$$w_s = -(\text{div}_{\text{H}})h \quad (9)$$

and the vertical velocity becomes proportional to height. Following Gryning and Batchvarova (1999) the horizontal divergence is estimated from the heating rate of the air in the free atmosphere as:

Table 1. Boundary-layer heights and potential temperatures determined from radio-soundings and aircraft measurements.

		Boundary-layer height (m)	Potential temperature (°C) at 2 km	RS: radiosounding AC: from aircraft
Hour UTC (12 June)	3:58		26.42	RS
	7:02	200	28.61	RS
	9:50	1000		AC
	10:09	1200	28.48	RS
	13:22	1400	29.91	RS
	16:39		29.97	RS
Hour UTC (13 June)	4:07		25.70	RS
	6:59	300	26.51	RS
	8:40	500		AC
	9:59	800	29.20	RS
	10:45	900		AC
	13:21	1600	30.21	RS
	16:08		30.53	RS

$$\mathrm{div}_\mathrm{H} = \left(\frac{d\theta(z)}{dt} \right) z^{-1} \gamma(z)^{-1} \qquad (10)$$

where $d\theta/dt$ is the rate of temperature increase in the free atmosphere at height z and γ the gradient of the potential temperature in the free atmosphere. For the experiments the horizontal divergence was estimated from $d\theta/dt$ and γ at 2 km, determined from the radio soundings (Table 2). The interpolation of the height of the boundary layer is illustrated in Fig. 3.

CO$_2$ concentrations within and above the boundary layer

The height of the atmospheric boundary layer can also been detected in the vertical profiles of the CO$_2$ concentrations that were measured by the airplane (Fig. 4). On both days, it could be seen that the CO$_2$ concentration inside the boundary layer was about 365 ppm and approximately constant with height. On 12 June, a jump of 5 ppm in the CO$_2$ concentration at 1000 meters height marked the top of the growing boundary layer. On 13 June, a jump in the CO$_2$ concentration at 500 meters indicated the top of the boundary layer. It can be seen that the next jump took place at about 1700 m which marks the top of the residual layer (top of boundary layer from the foregoing day). Above the residual layer the CO$_2$ concentration was about 380 ppm. The smaller concentration inside the boundary layer was caused by CO$_2$ uptake by the vegetation. The boundary layer heights on both days were in agreement with the estimate from the radiosonde measurements (Fig. 3). The measured CO$_2$ concentration at Lille Bøgeskov and RIMI are illustrated in Fig. 5.

Using the above parameters the regional fluxes were determined using Eq. 6. The results are shown in Fig. 6 and Table 3 together with the time series of the CO$_2$ fluxes near the ground at the RIMI site and above the deciduous forest at Lille Bøgeskov. It is evident that the regional flux of CO$_2$ in broad terms follows the behavior of the flux of CO$_2$ measured at RIMI (grassland) and Lille Bøgeskov (deciduous forest), and that the regional flux is comparable not only in size but also in the general diurnal (daytime) cycle of
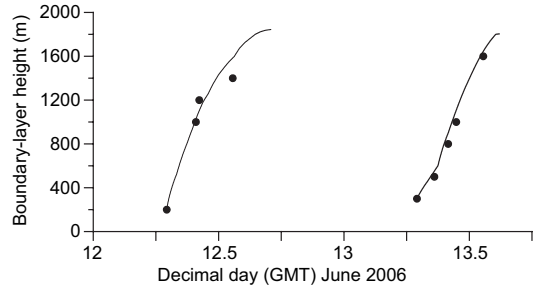

Fig. 3. Interpolated height of the boundary layer on 12–13 June 2006. Measurements are shown as bullets.

CO$_2$ fluxes at RIMI and Lille Bøgeskov. During daytime the integrated downward CO$_2$ flux over the beech forest was larger than over grassland indicating the important role of forest as a carbon sink (Fig. 6 and Table 3).

Discussion

Use of the budget method has as a necessary prerequisite that the effect of advection is negligible. Direct evaluation of the horizontal advection requires height precision measurements of the horizontal distribution of the CO$_2$ concentrations, which is not available in this experiment. The effect of horizontal advection on the daytime regional fluxes of CO$_2$ due to the inhomogeneous distribution of the surface vegetation was addressed by Wang *et al*. (2005). Their study was based on measurements of CO$_2$ at several towers in a forest. The overall estimate suggests that the impact of neglecting the horizontal advection on the daytime regional flux is 10%–15% of the flux during the growing season. Wang *et al*. (2005) and Feigenwinter *et al*. (2008) found that at night the effect can be substantial.

**Table 2**. Divergence of the horizontal wind velocity for the experiments on 12 and 13 June 2006.

Day and time (UTC)	10^5 div$_\mathrm{H}$ (s^{-1})
12 June 07:00–10:00	–0.1
12 June 10:00–13:00	1.1
12 June 13:00–16:00	0.04
13 June 07:00–10:00	1.39
13 June 10:00–13:00	0.47
13 June 13:00–16:00	0.18
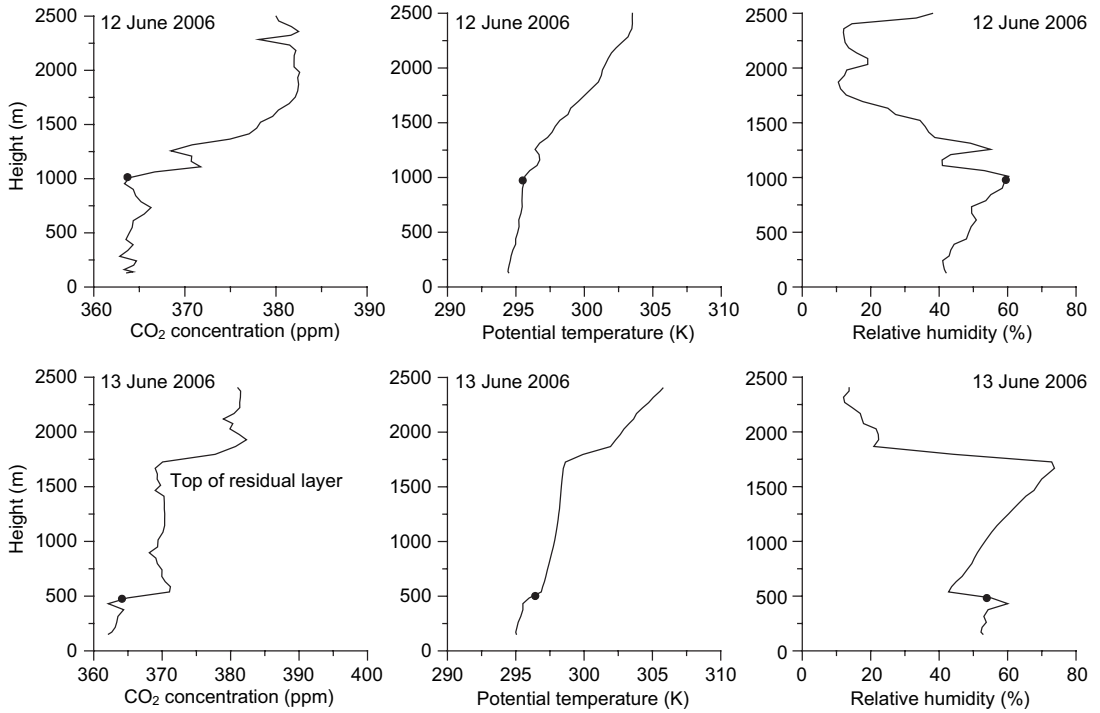
Fig. 4. CO_2 concentration, potential temperature and relative humidity profiles measured by the aircraft (12 June at around 09:50 GMT, and 13 June at around 08:40 GMT) near the RIMI site. The height of the boundary layer is indicated by the dots.
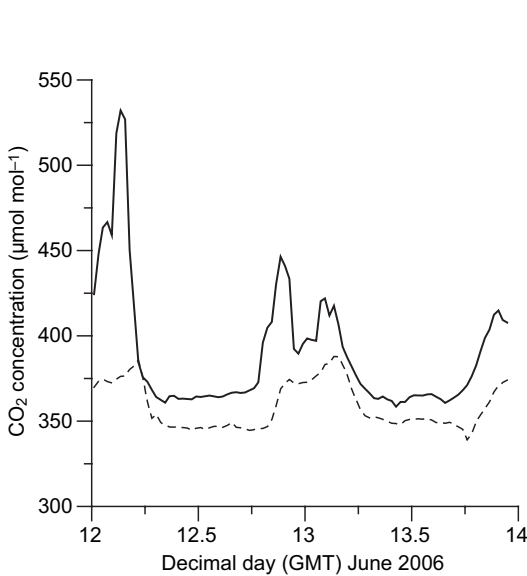
Fig. 5. CO_2 concentrations measured at RIMI at 2.5-m height (solid line) and Lille Bøgeskov at 43-m height (dashed line).
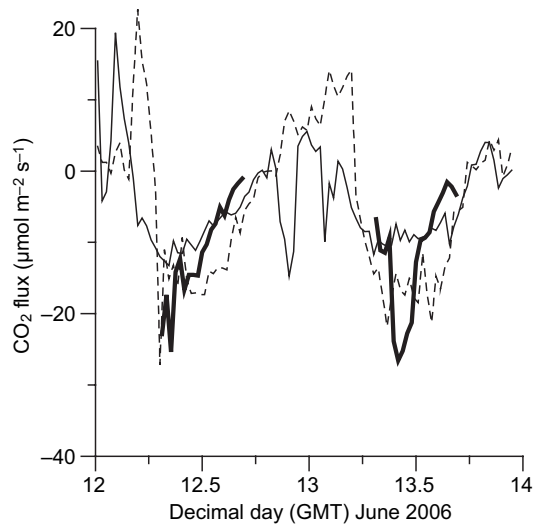
Fig. 6. CO_2 fluxes measured near the surface at RIMI/ grassland (thin solid line), Lille Bøgeskov/deciduous forest, (thin dashed line), and the regional CO_2 fluxes obtained with the boundary layer method (thick solid line).

Table 3. Average CO$_2$ fluxes (µmol m^{-2} s^{-1}).

Period 7:00 to 16:30 GMT	RIMI regional	RIMI agricultural grass point	Lille Bøgeskov deciduous forest point
12 June 2006	−11.1	−8.9	−14.2
13 June 2006	−11.5	−9.1	−15.6

Meteorological conditions during the experiment were typical for a well developed large-scale high pressure system, at both sites the wind speed was 3–4 m s^{-1} from southerly directions, a cloud-free sky and strong insolation resulted in a flux of ≈ 200 W m^{-2} around noon for the sensible heat, and > 300 W m^{-2} for the latent heat. In the afternoon, the temperature grew above 25 °C. Such conditions give rise to a considerable growth and development of a well defined top of the boundary layer and are, according to Wang *et al*. (2005), characterized by generally negligible advection. They are very favorable for the use of the budget method.

Information required for use of the boundary layer method is: (1) concentration of CO$_2$ at the surface, (2) vertical profiles of CO$_2$ concentration in order to estimate the jump in concentration at the top of the boundary layer, and (3) growth of the boundary layer. The boundary-layer method can be used to estimate CO$_2$ fluxes in areas where representative measurements are difficult to obtain (e.g., urban areas and over very inhomogeneous terrain such as mixed forest) (Batchvarova *et al*. 2001).

Measurements of CO$_2$ concentrations are standard at many places. The growth of the boundary layer can be obtained from wind speed and temperature profiles measured by radiosoundings when they are performed frequently enough to provide a reasonable detailed structure of the development of the boundary layer. Alternatively, data from remote sensing techniques can be used. The jump of the CO$_2$ concentration at the top of the atmospheric boundary layer can be measured by airplanes although this is costly. However, development of a CO$_2$ sensor that could be attached to a radiosonde and sensitive enough to measure the structure of the CO$_2$ profile would constitute a major scientific breakthrough in research of CO$_2$ aggregation.

References

Aubinet M., Grelle A., Ibrom A., Rannik U., Noncrieff J., Foken T., Kowalski A.S., Martin P.H., Berbigier P., Bernhofer C., Clement R., Elbers J., Granier A., Grunwald T., Morgenstern K., Pilegaard K., Rebmann C., Snijders W., Valentini R. & Vesala T. 2000. Estimates of the annual net carbon and water exchange of forests: The EUROFLUX methodology. *Adv. Ecol. Res*. 30: 113–175.

Batchvarova E. & Gryning S.E. 1991. Applied model for the growth of the daytime mixed layer. *Boundary-Layer Meteorol*. 56: 261–274.

Batchvarova E., Gryning S.E. & Hasager C.B. 2001. Regional fluxes of momentum and sensible heat over a sub-arctic landscape during late winter. *Boundary-Layer Meteorol*. 99: 489–507.

Betts A.K. 1973. Non-precipitating convection and its parameterization. *Q. J. R. Meteorol. Soc*. 99: 178–196.

Betts A.K. 1975. Parametric interpretation of trade-wind cumulus budget studies. *J. Atmos. Sci*. 32: 1934–1945.

Betts A.K. & Ball J.H. 1992. FIFE atmospheric boundary layer budgets methods. *J. Geophys. Res*. 97: 18525–18531.

Betts A.K. 1994. Relation between equilibrium evaporation and the saturation pressure budget. *Boundary-Layer Meterol*. 7: 235–245.

Bouwman A.F. 1999. *Approaches to scaling of trace gas fluxes in ecosystems*. Elsevier, New York.

Cao M. & Woodward F.I. 1998. Net primary and ecosystem production and carbon stocks of terrestrial ecosystems and their response to climate change. *Global Change Biol*. 4: 185–198.

Cramer W., Bondeau A., Woodward I., Prentice I., Betts R., Brovkin V., Cox P., Fisher V., Foley J., Friend A., Kucharik C., Lomas M., Ramankutty N., Sitch S., Smith B. & Young-Molling C. 2001. Global response of terrestrial ecosystem structure and function to CO$_2$ and climate change: results from six dynamic global vegetation models. *Global Change Biol*. 7: 357–373.

Dellwik E. & Jensen N.O. 2005. Flux-profile relationships over a fetch limited beech forest. *Boundary-Layer Meteorol*. 115: 179–204.

Denmead O.T., Raupach M.R., Dunin F.X., Cleugh H.A. & Leuning R. 1996. Boundary layer budgets for regional estimates of a scalar. *Global Change Biol.* 2: 255–264.

Ehleringer J.R. & Field C.B. 1993. *Scaling physological processes: leaf to globe*. Elsevier, New York.

Feigenwinter C., Bernhofer C., Eichelmann U., Heinesch B., Hertel M., Janous D., Kolle O., Lagergren F., Lindroth A., Minerbi S., Moderow U., Mölder M., Montagnani L., Queck R., Rebmann C., Vestin P., Yernaux M., Zeri M., Ziegler W. & Aubinet M. 2008. Comparison of horizontal and vertical advective CO_2 fluxes at three forest sites. *Agric. For. Meteorol.* 148: 12–24.

Gryning S.E. & Batchvarova E. 1999. Regional heat flux over the NOPEX area estimated from the evolution of the mixed layer. *Agric. For. Meteorol.* 98–99: 159–168.

Göckede M., Foken T., Aubinet M., Aurela M., Banza J., Bernhofer C., Bonnefond J.M., Brunet Y., Carrara A., Clement R., Dellwik E., Elbers J., Eugster W., Fuhrer J., Granier A., Grünwald T., Heinesch B., Janssens I. A., Knohl A., Koeble R., Laurila T., Longdoz B., Manca G, Marek M., Markkanen T., Mateus J., Matteucci G., Mauder M., Migliavacca M., Minerbi S., Moncrieff J., Montagnani L., Moors E., Ourcival J.-M., Papale D., Pereira J., Pilegaard K., Pita G., Rambal S., Rebmann C., Rodrigues A., Rotenberg E., Sanz M.J., Sedlak P., Seufert G., Siebicke L., Soussana J.F., Valentini R., Vesala T., Verbeeck H. & Yakir D. 2006. Quality control of CarboEurope flux data — Part I: Footprint analyses to evaluate sites in forest ecosystems. *Biogeosciences Discuss.* 4: 4025–4066.

Huntingford C., Cox P.M. & Lenton T.M. 2000. Contrasting responses of a simple terrestrial ecosystem model to global change. *Ecol. Model.* 132: 41–58.

Ibrom A., Dellwik E., Flyvbjerg H., Jensen N.O. & Pilegaard K. 2007a. Strong low-pass filtering effects on water vapour flux measurements with closed-path eddy correlation systems. *Agr. For. Meteorol.* 147: 140–156.

Ibrom A., Dellwik E., Larsen S.E. & Pilegaard, K. 2007b. On the use of the Webb-Pearman-Leuning theory for closed-path eddy correlation measurements. *Tellus B* 59: 937–946.

Joffre S.M., Kangas M., Heikinheimo M. & Kitaigorodskii S. 2001. Variability of the stable and unstable atmospheric boundary-layer height and its scales over a boreal forest. *Boundary-Layer Meteorol.* 99: 411–428.

Levy P.E., Grelle A., Lindroth A., Mölder M., Jarvis P.G., Kruijt B. & Moncrieff J.B. 1999. Regional-scale CO_2 fluxes over central Sweden by a boundary layer budget method. *Agric. For. Meteorol.* 98–99: 169–180.

Liu H.P., Peters G. & Foken T. 2001. New equations for sonic temperature variance and buoyancy heat flux with an omnidirectional sonic anemometer. *Boundary-Layer Meteorol.* 100: 459–468.

Mcnaughton K.G. & Spriggs T.W. 1986. A mixed-layer model for the regional evaporation. *Boundary-Layer Meteorol.* 34: 243–262.

Moore C.J. 1986. Frequency response corrections for eddy correlation systems. *Boundary-Layer Meteorol.* 37: 17–35.

Pilegaard K., Mikkelsen T.N., Beier C., Jensen N.O., Ambus P. & Ro-Poulsen H. 2003. Field measurements of atmosphere-biosphere interactions in a Danish beech forest. *Boreal Env. Res.* 8: 315–333.

Schlesinger M.E. 1983. A review of climate models and their simulation of CO_2-induced warming. *Int. J. Environ. Stud.* 29: 103–114.

Seibert P., Beyrich F., Gryning S.E., Joffre S., Rasmussen A. & Tercier P. 2000. Review and intercomparison of operational methods for the determination of the mixing height. *Atmos. Environ.* 34: 1001–1027.

Soegaard H., Jensen N.O., Bøgh E., Hasager C.B., Schelde K. & Thomsen A. 2003. A carbon dioxide exchange over agricultural landscape using eddy correlation and footprint modelling. *Agr. Forest Meteorol.* 114: 153–173.

Wang W., Davies K.J., Cook B.D., Bakwin P.S., Yi C., Butler M.P. & Ricciuto D.M. 2005. Surface layer CO_2 budget and advective contributions to measurements of net ecosystem–atmosphere exchange of CO_2. *Agric. For. Meteorol.* 135: 202–214.

Webb E.K., Pearman G.I. & Leuning R. 1980. Correction of flux measurements for density effects due to heat and water vapour transfer. *Q. J. Roy. Meteor. Soc.* 106: 85–100.

Wilczak J.M., Oncley S.P. & Stage S.A. 2001. Sonic anemometer tilt correction algorithms. *Boundary-Layer Meteorol.* 99: 127–150.